Solid State Science and Technology, Vol. 27, No 1 & 2 (2019) 75-88
ISSN 0128-7389 | *http://myjms.moe.gov.my/index.php/masshp*

PVP AIDED SYNTHESIS AND CHARACTERIZATION OF ZnO NANOPARTICLES

S. S. Abdullahi[1,2,4], *N.M. Saiden[2,3], J. Y.C. Liew[2,3], G.S.M Galadanci[4]

[1]*Physics Department, Federal University Dutse,*
P.M.B. 7156, Dutse, Jigawa State Nigeria

[2]*Physics Department, Faculty of Science, Universiti Putra Malaysia,*
43400 UPM Serdang, Selangor Malaysia

[3]*Institute of Advanced Technology, Universiti Putra Malaysia,*
43400 UPM Serdang, Selangor, Malaysia

[4]*Physics Department Bayero University, Kano Nigeria*
P.M.B.3011, Kano Nigeria

**Corresponding author:* nlaily@upm.edu.my

ABSTRACT

Zinc Oxide (ZnO) semiconductor nanoparticle aided with polyvinyl pyrrolidone (PVP) was synthesized using microwave assisted synthesis method. The structural, morphological, optical as well as the magnetic features of these nanoparticles were studied using X-ray diffraction (XRD), Field Emission Scanning Electron Microscopy (FESEM) UV-VIS spectroscopy, Photoluminescence (PL) spectroscopy and Vibrating Sample Magnetometer (VSM) respectively. The study attempt to tailor and observe the effect of PVP concentration to the structural, optical and magnetic properties of *ZnO* nanoparticles calcined at 600 ^{o}C. The PVP serve as a capping agent to avoid agglomeration and reduces the particle size. The result obtained show the formation of pure crystalline ZnO nanoparticles with the size ranged from 29-32 nm for the un calcined sample, while for the calcined samples, the crystallite size remain 43 nm for almost all the samples. FESEM images show a hexagonal nanorod structure with very little agglomeration. The band gap of the samples varies from 3.26- 3.31 and 3.25-3.26*eV* for both uncalcined and calcined sample respectively which show a blue shift when compared with the band gap of bulk ZnO material (3.37*eV*). The PL study for the calcined samples reveal the occurrence of three emission peak at 411, 459 and 528 nm. FTIR measurement confirms that the entire organic compound used was completely removed during the calcination. The magnetic measurement shows a diamagnetic behavior for the uncalcined, uncapped and PVP capped samples calcined at 600 ^{o}C.

Keywords: ZnO; PVP concentration; ZnO; structural; optical; magnetic properties

INTRODUCTION

The large surface area to volume ratio and size dependent effect of nanomaterials have gain much researchers' attention because of their effect on physical and chemical properties of materials [1]. Nanomaterials exhibit a recognizable optical, magnetic, mechanical, and electrical properties that are not possess by bulk materials [2].

Smaller particle size nanomaterials with homogeneous distribution can be achieved by introducing organic stabilizer as capping agent [3–5]. Polymer with polarity groups are versatile organic reagent used in the synthesis of nanomaterial especially metal oxides due to their biocompatibility with the metal ions [6]. Among the organic stabilizers, Polyvinylpyrrolidone (PVP) is one of the good candidates that play an important role in controlling the growth of nanomaterials. It prevent the agglomeration of the particles and enhance the degree of crystallinity of the nanomaterials, In addition, its concentration affect the morphology of the particles dispersant, it also act as a reducing agent and monitor the nucleation of the nanomaterials [3, 7].

Recent studies have shown that PVP can serve as a versatile reagent in the shape controlled synthesis of diluted magnetic semiconductor (DMS) the material in which a portion of nonmagnetic ions is replaced by a magnetic impurity of transition ions or rare earth metals ions which exhibit both ferromagnetic and semiconducting behavior [8,9,10]. These type of composites materials control the charge of the carriers and also manage its spin state which is needed for spin emitting diode, spin valve transistors, magnetic tunnel junction, spin memories etc [2, 11, 12].

Among the DMS, ZnO is one of the semiconducting materials with a wide band gap of $3.37eV$ and large exciting binding energy of $60meV$. Its good candidate due to its low cost, nontoxic, good chemical and thermal stability and also good magnetic property when doped with transition metals like Fe, Co, Ni, Mn. [9, 13, 14].

ZnO with PVP are types of composites materials which is processable and flexible with high mechanical strength, high thermal stability and also chemical resistance [15]. Mechanically, PVP stabilized the dissolved metallic salts through steric and electrostatic stabilization process on amide groups of pyrolidine rings and methylene groups. Ionic bond is formed between the metallic ions and the amide group of the polymeric chain. Consequently, the PVP decompose to some extent, thereby producing shorter polymer chains that are capped when adsorbed onto the surfaces of metallic ions [16, 17].

In this paper, PVP (40000) capping agent was used together with metallic nitrates to form a crystalline ZnO nanoparticles calcined at 600 ^{o}C. Different method have been employed for the synthesis of ZnO nanomaterials, these includes sol-gel [18, 19], hydrothermal, [2, 20] co precipitation [14–16], solid-state reaction [24], polymer pyrolysis route [10], and microwave assisted method [9, 25–28]. The microwave synthesis method is chosen due to its simplicity, versatility of the applied reaction condition, less time consumption, easy to apply and high chemical yield [9, 25–28].

EXPERIMENTAL

ZnO nanoparticle with different PVP concentration (0.0, 0.1, 1.0, 3.0g) were synthesized by microwave assisted synthesis method using an appropriate molar ratio of Zinc nitrate hexahydrate ($Zn(NO_3)_2.6H_2O$) as zinc precursor and PVP as capping agent. All chemicals used are analytical grade. Amount of PVP was completely dissolved in 20ml of distilled water using a magnetic stirer for 30 min. An appropriate molar ratio of $Zn(NO_3)_2.6H_2O$) was added in to the solution, the mixture was then stirred for 1hour until all the solute dissolved completely. NaOH was used to control the PH value at 12. The solution was placed in the microwave oven for 5 min at 380W, and allow to cool at room temperature. The precipitate formed will be centrifuged at 3000rpm and washed many times with distilled water followed by drying in an oven for 24 hour at 60 ^oC. The solid phase formed was finally grounded to form a nanoparticles. The powder was calcined at 600 ^oC for 2 hours at the rate of 3.1 ^oC /min.

The synthesised nanopowder was characterised by X-ray diffraction (XRD), Field Emission Scanning Electron Microscopy (FESEM). UV-VIS spectroscopy, Photoluminescence (PL) spectroscopy Fourier transform infrared spectroscopy (FTIR) and Vibrating Sample Magnetometer (VSM) respectively.

RESULTS AND DISCUSSION

Structural Analysis

X-ray diffraction was used to study the structural parameter and phase purity of the prepared ZnO samples. Figure1a and b show the diffraction pattern of ZnO nanoparticle prepared with 0.0, 0.1, 1.0 and 3.0g PVP for the uncalcined and calcined at 600 ^oC respectively. Both patterns display a hexagonal structure ZnO where all the diffraction peak match well to the hexagonal phase of ZnO with space group P63mc and space number 186 (ICSD). The following prominent peaks (100), (002), (101), (102), (110), (103), (200), (112), (201), (004), and (202) were present in all the samples, where the most intense peak appeared at (101) for all samples, For the uncalcined samples there is a presence of $NaNO_3$ as impurity observed for 1.0 and 3.0g PVP which results from the precursors used. However, the impurities disappeared when calcination temperature is applied. This confirms the formation of pure crystalline ZnO structure at 600 ^oC. It reveals that at high calcination temperature of 600 ^oC the PVP does not alter the crystal structure as the peaks are identical, [29]. For the uncalcined sample the intensity of the peak decreases with an increase in the PVP concentration however the intensity becomes sharper when the calcination temperature is applied, this indicates that there is an intensification in the crystallinity of the samples at this calcination temperature [30].

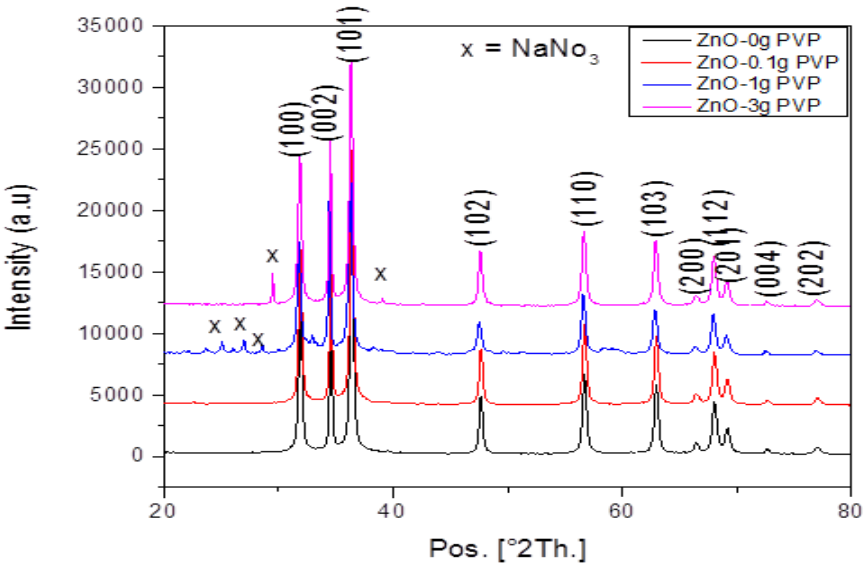

(a) Uncalcined

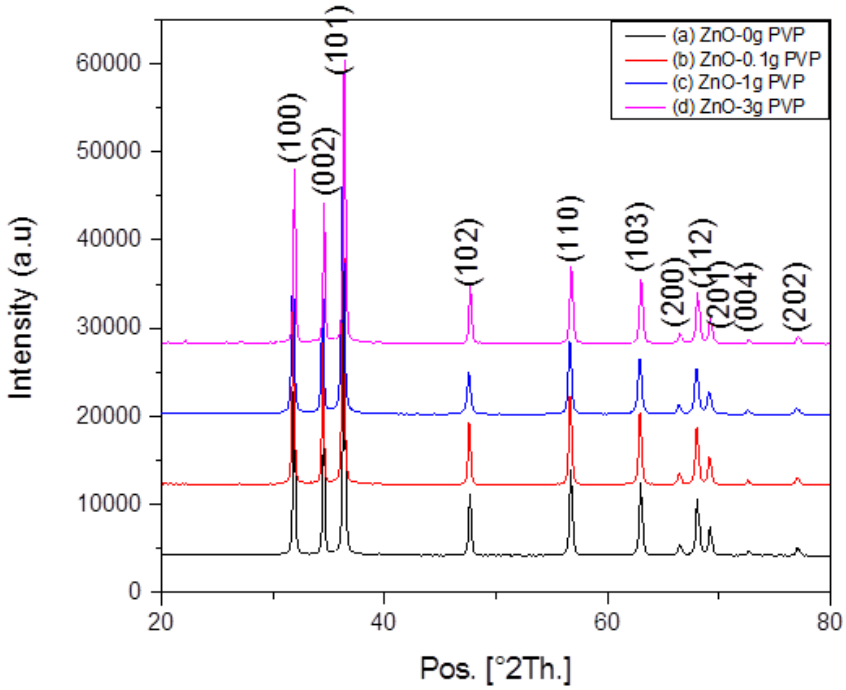

(b) Calcined

Figure 1: X-ray diffraction pattern of ZnO at different concentration of PVP (0.0, 0.1, 1.0, 3.0g) (a)Un calcined (b) Calcine at 600 ^{o}C

The crystallite size of these samples were calculated using Scherer's equation [23, 31, 32].

$$D = \frac{k\lambda}{\beta cos\theta} \quad \text{.....(1)}$$

The crystallite size of the samples before and after calcination has been tabulated in table 1. For the calcined samples, there is a general increment in the size of the nanoparticle as compared to the uncalcined sample, this is due to the increase in the intensity of the peaks and also a decrease in the FWHM of the peak as a result of calcination effect [33, 34]. At high temperature, the thermal calcination forces merging of the nanoparticles which lead to the increment in the size of the nanoparticle [29]. However for the uncalcined sample there is a reduction in the size of the particles as a result of the concentration of PVP meanwhile there is a deviation in the size of the sample shown by 1.0g PVP this is due to the impurity observed in the sample which causes a strain induced in the particles thereby increasing the size of the particles. The most intense peak for the uncalcined samples decrease from 21031.63 to 14568.45 with an increase in the PVP. This is what bring about the reduction in the size of the particle [20]. The reduction is due to the strong coordination ability of the polar group in the pyrrolidone ring which causes a strong interaction between the PVP and the surface of the particle, moreover shell can be formed over the particle surface reducing the aggregation as well as the size of the particles [3]. The decreases in size with an increase in the PVP concentration also confirms that PVP control the growth of the nanoparticles and inhibit their nucleation [7].

The lattice parameters *a*, *c* and also the volume of the unit cell is calculated using equations *2* and *3* respectively [10, 11, 23, 32].

$$\frac{1}{d^2} = \frac{4}{3}\left(\frac{h^2+hk+k^2}{a^2}\right) + \frac{l^2}{c^2} \quad \text{.....(2)}$$

$$V = 0.866a^2c \quad \text{.....(3)}$$

Table 1: Crystallite size of the samples before and after calcination

Samples (g)	Before calcination						After Calcination at 600 °C					
	Height of the most intense peak	Crystallites size (nm)	c (002)	a (110)	V (A^3)	c/a	Height of the most intense peak	Crystallites size (nm)	C (002)	a(110)	V (A^3)	c/a
$PVP_{0.0}$ /ZnO	21031.6	32	5.1859	3.2439	47.26	1.599	32964.4	43	5.1859	3.2439	47.26	1.599
$PVP_{0.1}$ /ZnO	20393.9	29	5.1859	3.2446	47.28	1.598	34973.8	43	5.1964	3.2473	47.45	1.600
$PVP_{1.0}$ /ZnO	14568.5	32	5.2051	3.2507	47.63	1.601	27860.8	37	5.2034	3.2487	47.56	1.602
$PVP_{3.0}$ /ZnO	19707.0	29	5.1929	3.2473	47.42	1.599	32331.6	43	5.1824	3.2418	47.17	1.599

The lattice parameters increase slightly with an increase in PVP concentration for both the uncalcined and calcined sample with the exception of 3.0g PVP which shows a sudden fall in the lattice parameter, This might be as a result of the large amount of the PVP used that induces strain in the crystal lattice of ZnO. Similarly, the volume of all the samples increases with an increase in the PVP concentration. The ratio of the lattice parameter *c/a* is having an approximate value of 1.60 for all the samples which is almost the same with the standard value of ZnO (*c/a* to be 1.62). This confirms that PVP and the calcination temperature of 600 ^{o}C has no much effect on the overall structure of ZnO [10, 11].

Optical properties

UV Visible spectroscopy was used to study the optical properties of the prepared samples. Figure 2a & b show the diffused reflectance (DR) spectra of the PVP capped *ZnO* uncalcined and calcined samples measured in the wavelength range of 200–800nm. All the spectra show an absorption edge below 380nm and least intensity above 70%. For the uncalcined sample the intensity decreases with the concentration of PVP except for 0.1g and 3.0g PVP where the intensity reaches 95% for uncalcined and calcined sample respectively. Kubelka Munk was used to calculate the band gap of the prepared samples as presented in equation *4* and *5* [12, 35, 36].

$$F(R) = \frac{(1-R)^2}{2R} \quad \text{.....4}$$

$$F(R)E = (hv - E_g)^n \quad \text{.....5}$$

of reflectance (i. e. *R/100*), hv is the photon energy and E_g is the band gap. The optical band gap was calculated by extrapolating the linear part $(F(R)E)^2$ versus *E* (hv) curve to zero as shown in Figure 3. The estimated band gap energies for the 0.0g, 0.1g, 1.0g and 3.0g PVP capped ZnO were 3.24, 3.3, 3.26, 3.31*eV* and 3.25, 3.25, 3.26. 3.26*eV* for the uncalcined and calcined sample respectively. For the uncalcined samples the band gap increases for the increase in the PVP concentration. However after the calcination the band gap remain almost constant with value ranged from 3.25-3.26 *eV*. The band gap energy of PVP capped ZnO nanoparticles for the uncalcined and calcined samples show the blue shift as compared to bulk ZnO (3.37*eV*) [36].

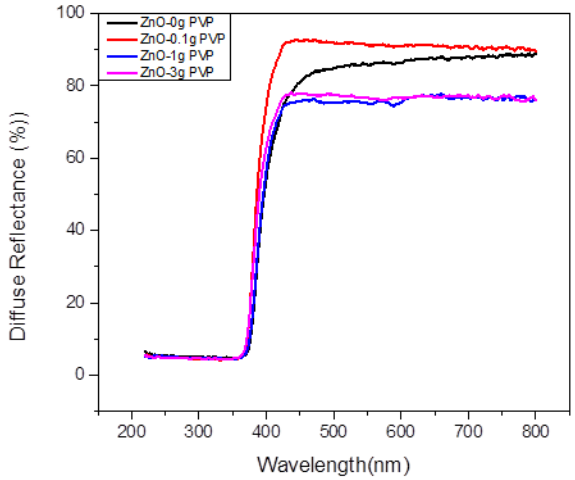

(a) Uncalcined

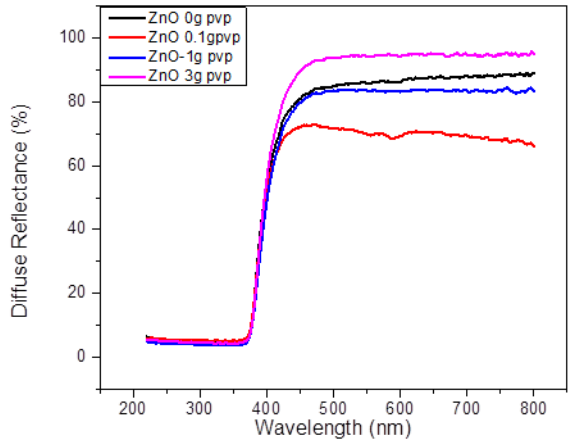

(b) Calcined

Figure 2: Diffuse reflectance spectra of different concentration of PVP (0.0, 0.1, 1.0, 3.0g) (a) Uncalcined (b) Calcined at 600 ^{o}C

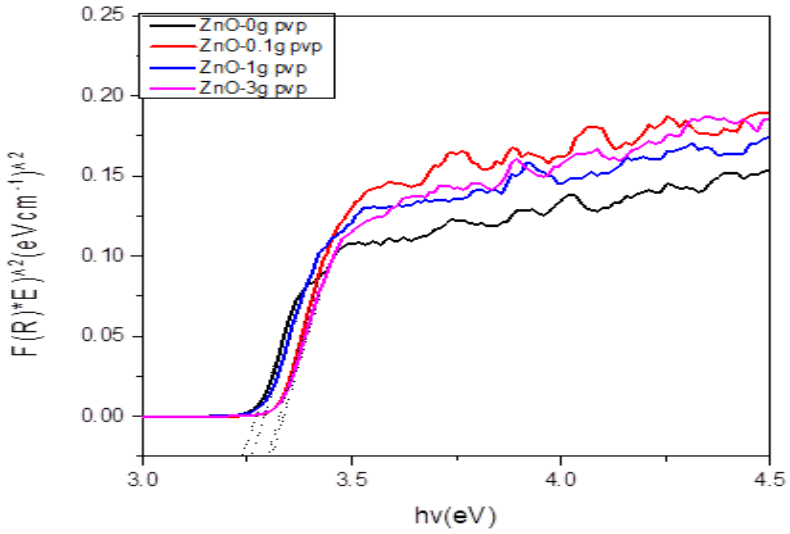

(a) Uncalcined

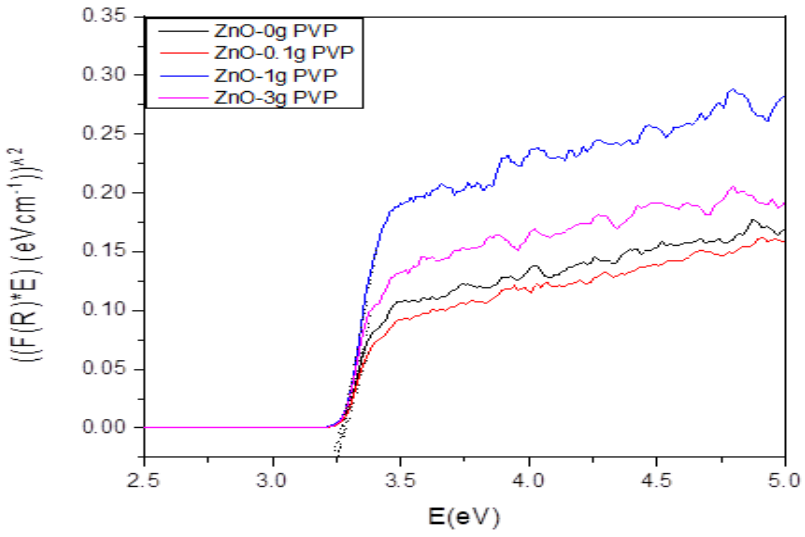

(b) Calcined

Figure 3: Tauc plot of *(F(R)xE)^2* versus *E* of different concentration of PVP (0.0, 0.1, 1.0, 3.0g) (a) Un calcined (b) Calcined at 600 ^{o}C

Photoluminescence analysis

Photoluminescence (PL) spectroscopy is a tool use to study the optical properties that are related to intrinsic and extrinsic defects in semiconductors. It also provides information about the energy states of impurities and defects. Figure 4 shows the room temperature photoluminescence spectra for the uncapped and PVP capped ZnO

nanoparticles calcined at 600 ^{o}C with the excitation wavelength of 325 nm. The spectra demonstrated the appearance of three emission peaks at 411 nm, 459 nm and 528 nm. The 411 nm peak corresponds to a violet band. This emission is due to the near band edge emission as a result of the excitation recombination [37, 38]. The 459 nm peak corresponds to a blue band emission which indicate the presence of zinc interstitial related defect in the samples [37]. The 528 nm peak corresponds to green emission due to recombination of the photogenerated carrier occupying the oxygen vacancy [39, 40]. The low PL intensity shows low recombination rate of charge carriers indicating high usage of the electron hole pair in the material. The position of the peaks are the same for all the samples, however their intensities differs. The uncapped sample shows the highest intensity which decreases with PVP concentration. This indicates that the PVP does not have much effect in the emission of the synthesized samples [15]. In principle, the intensity of the PL spectra represents recombination efficiency of electron-hole pairs, the highest intensity indicates the greatest electron-hole recombination efficiency resulted in the lowest photodegradation efficiency [40].

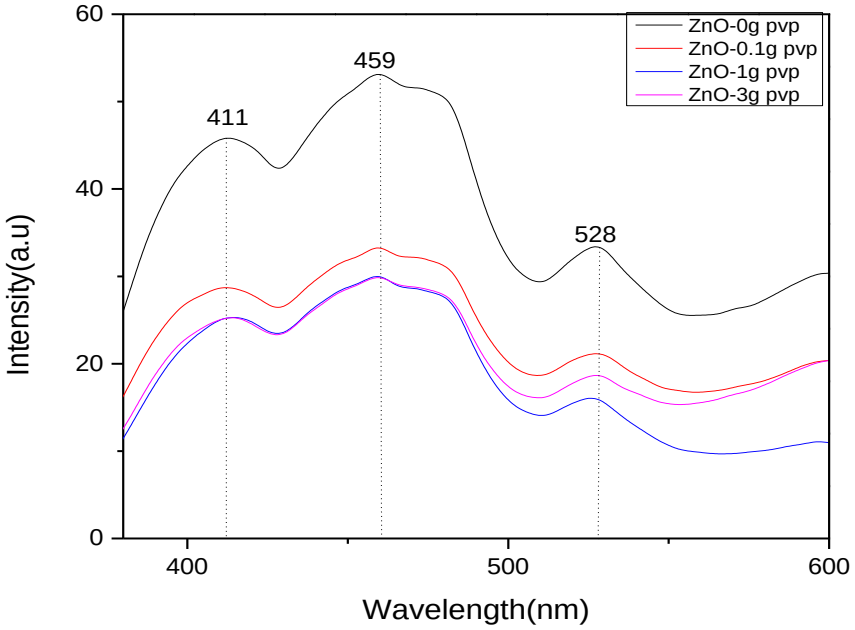

Figure 4: Room temperature Photoluminescence spectra of ZnO calcined at 600 ^{o}C for different concentration of PVP (0.0, 0.1, 1.0, 3.0g)

Field Emission Scanning Electron Microscopes (FESEM)

The morphology of the samples was measured by field emission scanning electron microscopes (FESEM). Figure 5 shows the images of 1g PVP capped ZnO nanoparticle at different magnification. The images reveal the formation of hexagonal shaped ZnO nanorods with a non-uniformly distributed nanoparticle, their diameter ranged from 12 nm to 35 nm. There is not much agglomeration observed in the images as distinct

boundary between neighboring crystallites can still be observed. This result confirms the XRD results [41, 42].

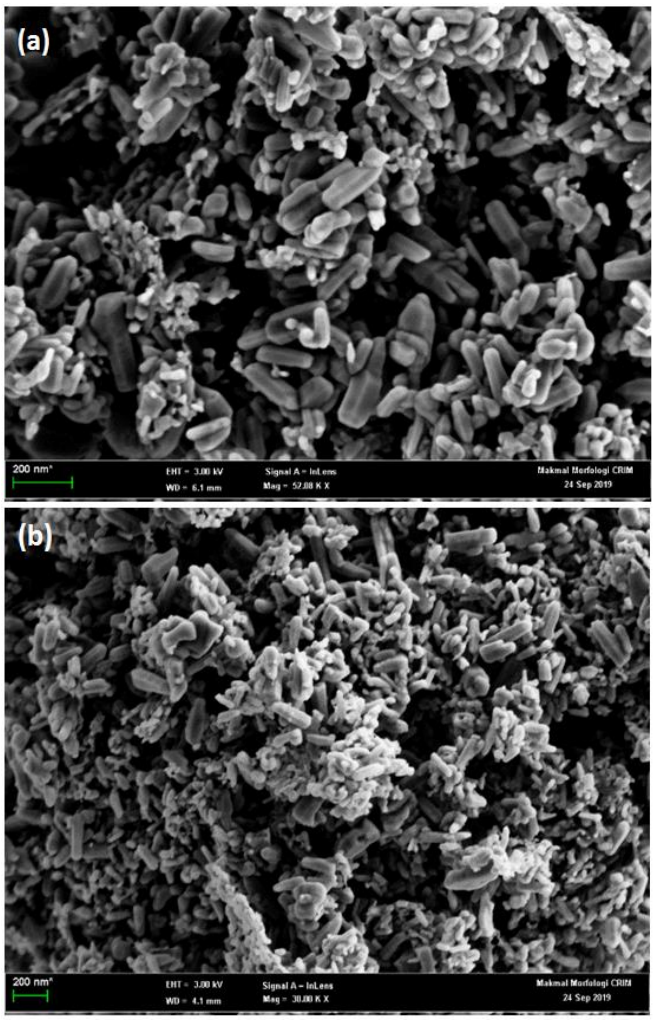

Figure 5: FESEM images of calcined 1g PVP capped ZnO nanoparticles (a) 5200k x (b) 3200k x

FTIR measurement

The FTIR spectrum of uncapped and PVP capped ZnO nanoparticles calcined at 600 ^{o}C is presented in the range of 400cm^{-1} to 40000cm^{-1} as shown in Figure 6. All the samples demonstrate a band around 3404cm^{-1} which corresponds to O-H stretching as a result of the absorbed water, the intensity of the peak decreases with an increase in the PVP concentration. Similarly, there is an appearance of peaks around 1550cm^{-1} and 1417cm^{-1} which correspond to C-O asymmetrical and symmetrical stretching of the zinc carboxylate respectively. A band around 1020cm^{-1} and 839cm^{-1} are due to ZnO associated with C-O vibration and tetrahedral coordinate of Zn respectively [45, 46]. Moreover a highly intense peak around 550cm^{-1} represent a stretching mode of ZnO, the

band shift toward lower wavenumber as a result of the increase in the PVP concentration. This confirm that the PVP is chemically absorbed to ZnO surface through the carboxyl group [15].

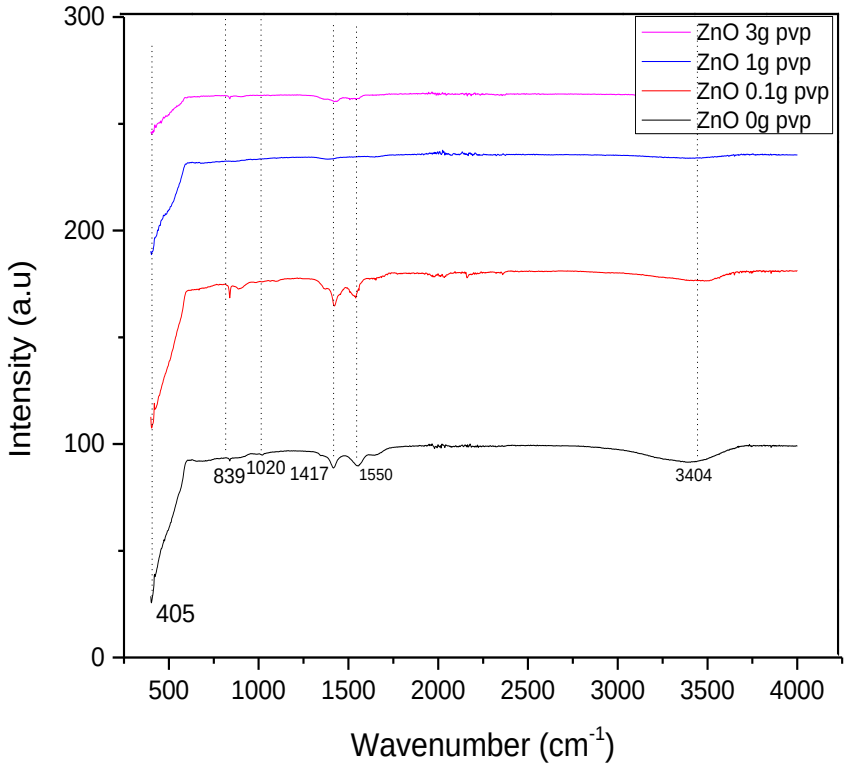

Figure 6: FTIR of uncapped and PVP capped ZnO nanoparticles calcined at 600 ^{o}C

Magnetic measurement

Vibrating sample magnetometer was used to identify the magnetic feature of the samples. Figure 7 shows the magnetic graph of the uncapped and PVP capped ZnO nanoparticles calcined at 600 ^{o}C measured at room temperature in the magnetic field range from 0 to ±15,000G. The hysteresis reveals that all the samples present a diamagnetic behavior similar to the bulk ZnO. We can infer from the graph that there is no magnetic transition as a result of the PVP and also the calcination temperature. Similar result is observed for undoped ZnO samples prepared by different methods [9 , 21, 32, 43, 44].

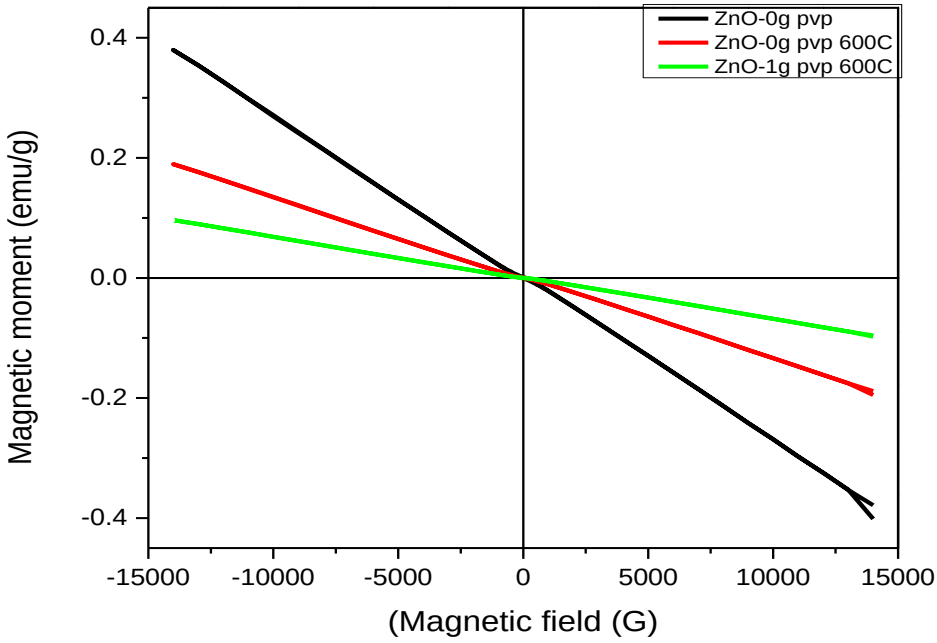

Figure 7: RT magnetic measurement of uncapped and 1.0g PVP capped ZnO nanoparticles calcined at 600 ^{o}C

CONCLUSION

Microwave assisted synthesis method was used to synthesized the uncapped and PVP capped ZnO nanoparticles calcined at 600 ^{o}C. The result obtained for the calcined sample shows a formation of pure crystalline ZnO nanoparticles with a hexagonal nanorod structure, however, the presence of $NaNO_3$ as impurity is observed for the uncalcined sample with 1.0 and 3.0g PVP. The band gap of both samples show a blue shift when compared with the bulk ZnO material, PL result for the calcined sample shows three emission peak occurred at 411, 459 and 528 nm for all the samples. FTIR measurement confirms that the PVP were completely removed during the calcination. The magnetic measurement reveals a diamagnetic behavior for both uncapped and PVP capped sample calcined at 600 ^{o}C. We can inferred from the results that for the un calcined samples the PVP concentration affect the size of the particles as well as its band gap, However for the calcined sample there is an intensification in the crystallinity of the samples but their size as well as the band gap remain almost constant.

ACKNOWLEDGEMENT

The Author acknowledges Federal Government of Nigeria for their financial commitment toward the whole project.

REFERENCES

[1] M. Goodarz Naseri, E. Bin Saion, H. A. Ahangar, M. Hashim, and A. H. Shaari, *J. Magn. Magn. Mater.*, **323** (13) 1745–1749 (2011)
[2] T. C. Bharat, Shubham, S. Mondal, H. S.Gupta, P. K. Singh, and A. K. Das, *Mater. Today Proc.*, **11** 767–775 (2019)
[3] K. M. Koczkur, S. Mourdikoudis, L. Polavarapu, and S. E. Skrabalak, *Dalt. Trans.*, **44** (41) 17883–17905 (2015)
[4] Y. Yuliah and A. Bahtiar, *AIP Conf. Proc.*, **1554** 139–142 (2013)
[5] G. Murugadoss, *J. Mater. Sci. Technol.*, **28** (7) 587–593 (2012)
[6] P. R. Patil and S. S. Joshi, *Mater. Chem. Phys.*, **105** (2–3) 354–361 (2007)
[7] H. A. Ahmad, N. M. Saiden, E. Saion, R. S. Azis, M. S. Mamat, and M. Hashim, *J. Magn. Magn. Mater.*, **428** 219–222 (2017)
[8] R. Silva, A. Ferreira, and R. Kishore, "Ferromagnetism in Dilute Magnetic Semiconductors," pp. 12–16.
[9] "Synthesis and characterization of Mn and Co codoped ZnO nanoparticles," no. July, 2015.
[10] A. H. Farha, S. A. Mansour, and M. F. Kotkata, *J. Mater. Sci.*, **51** (21) 9855–9864 (2016)
[11] N. K. Singh, V. Koutu, and M. M. Malik, "Enhancement of room temperature ferromagnetic behavior of Co-doped ZnO nanoparticles synthesized via sol–gel technique," *J. Sol-Gel Sci. Technol.*, 2019.
[12] M. Asemi, B. Mortezapour, and M. Ghanaatshoar, *J. Supercond. Nov. Magn.*, **32** (2) 269–275 (2019)
[13] R. Elilarassi and G. Chandrasekaran, *J. Mater. Sci. Mater. Electron.*, **21** (11) 1168–1173 (2010)
[14] J. M. Zhang, D. Gao, and K. W. Xu, *Sci. China Physics, Mech. Astron.*, **55** (3) 428–435 (2012)
[15] V. C. Agulto *et al.*, *Opt. Mater. (Amst).*, **76** 317–322 (2018)
[16] A. H. Naseri, M. G, Saion, E. B., Shaari, *Int. Nano Lett.*, **3** 1–19 (2013)
[17] P. L. Leng, M. G. Naseri, E. Saion, A. H. Shaari, and M. A. Kamaruddin, *Adv. Nanoparticles*, **2** (4) 378–383 (2013)
[18] K. Irshad, M. T. Khan, and A. Murtaza, *Phys. B Condens. Matter*, **543** 1–6 (2018)
[19] M. Ravindiran and P. Shankar, *J. Mater. Sci. Mater. Electron.*, **28** (5) 4229–4238 (2017)
[20] H. Kamari *et al.*, *Crystals*, **7** (2) 2 (2017)
[21] G. Vijayaprasath *et al.*, *Appl. Phys. A Mater. Sci. Process.*, **122** (2) 1–11 (2016)
[22] T. Thangeeswari, M. Priya, and J. Velmurugan, *J. Mater. Sci. Mater. Electron.*, **26** (4), 2436–2444 (2015)
[23] R. P. Pal Singh, I. S. Hudiara, S. Panday, and S. B. Rana, *J. Supercond. Nov. Magn.*, **29** (3) 819–827 (2016)
[24] S. A. Ahmed, *Appl. Phys. A Mater. Sci. Process.*, **123** (6) 1–9 (2017)
[25] G. Sankar, "Preparation of nano phosphors by Microwave-assisted combustion synthesis," vol. 7560, pp. 86–89.

[26] L. C. Nehru and C. Sanjeeviraja, "Microwave-assisted combustion synthesis of nanocrystalline ZnO powders using zinc nitrate and various amount of organic fuels as reactants : influence of reactant parameters- A status review," vol. 6, pp. 75–110, 2014.
[27] M. R. De Freitas, G. L. De Gouveia, J. A. De Oliveira, R. Herta, and G. Aliaga, "Microwave Assisted Combustion Synthesis and Characterization of Nanocrystalline Nickel-doped Cobalt Ferrites," vol. 19, pp. 27–32, 2016.
[28] A. Baykal and Y. Ko, "Microwave-assisted combustion synthesis of CoFe 2 O 4 with urea , and its magnetic characterization," vol. 57, pp. 441–444, 2007.
[29] Z. N. Kayani, F. Saleemi, and I. Batool, *Appl. Phys. A Mater. Sci. Process.*, **119** (2) 713–720 (2015)
[30] M. Goodarz Naseri, E. B. Saion, H. Abbastabar Ahangar, A. H. Shaari, and M. Hashim, "Simple synthesis and characterization of cobalt ferrite nanoparticles by a thermal treatment method," *J. Nanomater.*, vol. 2010, 2010.
[31] B. Babu, V. P. Manjari, T. Aswani, G. T. Rao, R. J. Stella, and R. V. S. S. N. Ravikumar, *Indian J. Phys.*, **88** (7) 683–690 (2014)
[32] R. Krithiga, S. Sankar, and V. Arunkumar, *J. Supercond. Nov. Magn.*, 29 (1) 245–251 (2016)
[33] R. Hariharan, S. Senthilkumar, A. Suganthi, and M. Rajarajan, *J. Photochem. Photobiol. A Chem.*, **252** 107–115 (2013)
[34] M. Molla, M. Furukawa, I. Tateishi, H. Katsumata, and S. Kaneco, *J. Compos. Sci.*, **3** (1) 18 (2019)
[35] R. Peña-Garcia *et al.*, *Ceram. Int.*, **45** (1) 918–929 (2019)
[36] R. N. Ali, H. Naz, J. Li, X. Zhu, P. Liu, and B. Xiang, *J. Alloys Compd.*, **744** 90–95 (2018)
[37] A. Kalita and M. P. C. Kalita, *Opt. - Int. J. Light Electron Opt.*, **130** 955–962 (2017)
[38] H. Ji, C. Cai, S. Zhou, and W. Liu, *J. Mater. Sci. Mater. Electron.*, **29** (15) 12917–12926 (2018)
[39] S. Lam, M. Kee, and J. Sin, "In fl uence of PVP surfactant on the morphology and properties of ZnO micro / nano fl owers for dye mixtures and textile wastewater degradation," vol. 212, pp. 35–43, 2018.
[40] S. Kakarndee and S. Nanan, *J. Environ. Chem. Eng.*, **6** (1) 74–94 (2018)
[41] Y. Caglar, K. Gorgun, and S. Aksoy, *Spectrochim. ACTA PART A Mol. Biomol. Spectrosc.*, **138** 617–622 (2015)
[42] B. Poornaprakash, U. Chalapathi, M. Kumar, and P. T. Poojitha, *J. Mater. Sci. Mater. Electron.*, **29** (3) 2316–2321 (2018)
[43] T. Thangeeswari, P. Murugasen, and J. Velmurugan, *J. Supercond. Nov. Magn.*, **28** (8) 2505–2515 (2015)
[44] S. B. Rana, R. P. P. Singh, and S. Arya, *J. Mater. Sci. Mater. Electron.*, **28** (3) 2660–2672 (2017)
[45] R. Javed, M. Usman, S. Tabassum, and M. Zia, *Appl. Surf. Sci.*, **386** 319–326 (2016)
[46] S. Choudhary and R. J. Sengwa, *Curr. Appl. Phys.*, **18** (9) 1041–1058 (2018)